J. Biochem. **134**, 661–666 (2003)
DOI: 10.1093/jb/mvg190

Intermolecular Contact Regions in Urokinase Plasminogen Activator Receptor

Olin D. Liang*[,1], Khalil Bdeir[2], Rachel L. Matz[1], Triantafyllos Chavakis[3] and Klaus T. Preissner[1]

[1]Institut für Biochemie, Fachbereich Humanmedizin, Justus-Liebig-Universität, Friedrichstr. 24, D-35392 Giessen, Germany; [2]Department of Pathology and Laboratory Medicine, University of Pennsylvania, 422 Curie Blvd. Philadelphia, Pennsylvania 19104, USA; and [3]Medizinische Klinik und Poliklinik I, Universitätsklinikum, Bergheimerstr. 58, D-69115 Heidelberg, Germany

Received August 18, 2003; accepted August 22, 2003

The glycolipid-anchored urokinase-type plasminogen activator receptor (uPAR) is engaged in various signal transduction events related to cell adhesion, migration and proliferation. In this study, using phage display and peptide array techniques, we have identified several intermolecular contact regions of uPAR. Phage-displayed uPAR fragments bound to immobilized soluble uPAR on magnetic beads, revealing that regions uPAR-(7–28) and uPAR-(60–91) in domain I, uPAR-(101–121) in domain II and uPAR-(240–260) in domain III are possible uPAR-uPAR contact sites. Using peptide array, two additional sites could be identified, uPAR-(51–59) in domain I and uPAR-(144–155) in domain II. The putative uPAR-uPAR interaction sites are different from the previously identified uPA-binding sites. Functionally, peptides uPAR-(84–95) and uPAR-(240–248) could partially inhibit differentiated human U937 monocyte adhesion to vitronectin in the presence of uPA, indicating that these two uPAR regions might be involved not only in uPAR-uPAR but also in uPAR-vitronectin interactions. We propose that multiple uPAR-uPAR ectodomain interactions contribute considerably to the regulation of various cellular functions of uPAR.

Key words: extracellular matrix protein, uPA, uPAR.

Abbreviations: uPA, urokinase-type plasminogen activator; uPAR, uPA receptor; suPAR, soluble uPAR; Vn, vitronectin; GPI, glycosyl-phosphatidylinositol.

Extracellular proteolysis plays a key role in biological processes in the vascular system related to, *e.g.*, angiogenesis, wound healing, fibrinolysis, vascular remodeling and tumor metastasis. Together with the expression and functions of various adhesion molecules, the extent of cell adhesion, migration and invasion depends largely on coordination between cell-associated adhesive and proteolytic systems. Urokinase-type plasminogen activator (uPA) is a serine proteinase that interacts with its cell surface receptor, and the binding initiates a cascade of pericellular proteolysis as well as receptor activation (*1*). The urokinase plasminogen activator receptor (uPAR) was originally identified as the cell surface receptor for the serine proteinase. The mature form of the human receptor consists of 283 amino acid residues organized into three homologous domains (DI, DII and DIII) that associate with the membrane through a glycosylphosphatidylinositol (GPI) anchor at the C-terminus (*1*). uPAR has been linked to cellular adhesion, proliferation and migration through its capacity to promote pericellular proteolysis, regulate integrin functions, and mediate cell signaling in response to uPA binding (*2*, *3*). The mechanisms for these activities remain incompletely defined, although uPAR is now considered to be a cis-acting ligand for β1, β2, and β3 integrins (*4–6*). A recent study demonstrated that uPAR is a β1- and β3-integrin ligand and binds specifically to integrins on opposing cells, suggesting that the uPAR-integrin interaction may mediate cell-cell (trans-) interaction (*7*).

Dimerization/oligomerization is the mechanism responsible for receptor activation of most, if not all, transmembrane receptors. Receptors attached to the membrane by a GPI-anchor, on the other hand, cluster in particular membrane microdomains, known as lipid rafts, where they may make contact with various signal molecules (*8*, *9*). Accumulating evidence supports the hypothesis that uPAR molecules form functional dimers/oligomers. uPAR has been shown to be associated with the components of the JAK1/STAT1 signaling pathway and can cause activation of this pathway upon receptor clustering in the human kidney epithelial tumor cell line TCL-598 (*10*). In another study, the clustering of uPAR induced proinflammatory signaling in human polymorphonuclear neutrophils (*11*). A recent report demonstrated ligand-induced uPAR oligomerization (*12*). All these observations have extensive implications for GPI-anchored receptors in general and for the biology of the uPA/uPAR system in particular. The aim of this study was to identify putative intermolecular contact regions of uPAR and to explore the possible function of these regions.

*To whom correspondence should be addressed. Tel: +49-641-99-45180, Fax: +49-641-99-47509, E-mail: olin.d.liang@biochemie.med.uni-giessen.de

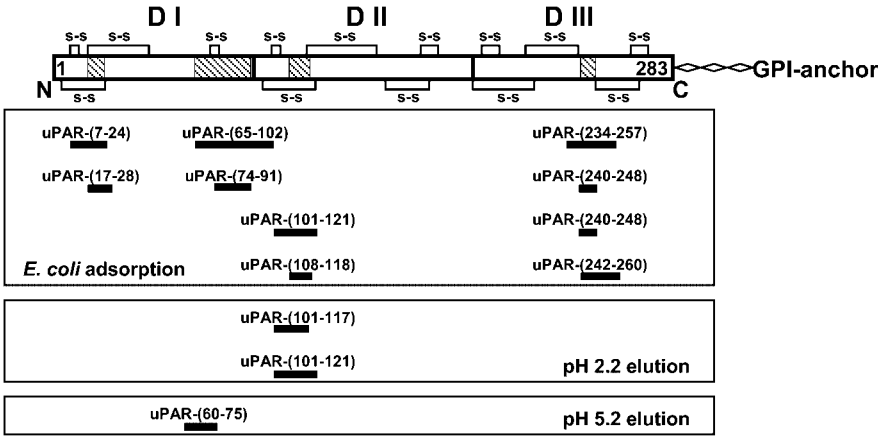

Fig. 1. **Alignment of uPAR-binding uPAR peptides.** The peptides were obtained after pH 5.2 elution, pH 2.2 elution and *E. coli* adsorption.

MATERIALS AND METHODS

Materials—The plasmid pBSW87 containing the full-length uPAR cDNA was obtained from Dr. N. Behrendt (Finsen Laboratory, Copenhagen, Denmark). The phagemid vector pComb3B was obtained from Dr. H. Pannekoek (Academic Medical Center, Amsterdam, The Netherlands). The VCSM13 interference-resistance helper phage and the electroporation competent *E. coli* XL-1 Blue MRF′ were purchased from Stratagene (Amsterdam, The Netherlands). The *Bst*XI linker was from Invitrogen (Groningen, The Netherlands). Recombinant human suPAR from insect cells was a gift from Dr. D. Cines (University of Pennsylvania, Philadelphia, PA). All other chemicals and reagents were of analytical grade.

Affinity Selection of suPAR-Binding Phagemid Particles and Sequencing of cDNA Fragment Inserts—Construction and characterization of a uPAR random epitope phage library as well as affinity selection of suPAR-binding phagemid particles were performed as described previously (*13*, *14*). Briefly, human suPAR was coated onto tosylactivated Dynalbeads M-280 (Dynal, Hamburg, Germany) according to the manufacturer's instructions, and the suPAR-coated beads (approximately 5 μg suPAR per 10^8 beads in 1 ml) were stored in phosphate-buffered saline (PBS) containing 0.1% (w/v) bovine serum albumin (BSA) and 0.02% sodium azide at 4°C. After washing three times in PBS, 100 μl uPAR-coated magnetic beads were blocked with 1.5 ml PBS containing 3% BSA and 0.05% Tween-20 (PBST-3% BSA) for 1.5 h at room temperature. The beads were then resuspended in 50 μl PBST-3% BSA and mixed with 50 μl of the uPAR phage display library in PBST-3% BSA containing 1.6×10^{10} phagemid particles for 2 h at room temperature with gentle agitation. After binding, the bead suspension was transferred into a fresh 1.5 ml Eppendorf tube to avoid plastic bound phagemid particles. With the help of a magnetic particle concentrator (Dynal MPC-E-1), the beads carrying uPAR-binding phages were washed ten times with PBST-3% BSA and resuspended in 200 μl 0.3 M NaAc buffer, pH 5.2. After a short vortexing step, the supernatant was removed and immediately neutralized by adding 12 μl 2M Tris buffer, pH 10.5. The eluted phagemid particles were used to infect 100 μl of freshly cultured *E. coli* XL-1 Blue MRF′ cells at 37°C for 20 min. Subsequently, the paramagnetic beads were incubated in 200 μl 0.1 M glycine-HCl buffer, pH 2.2, and the eluted phagemid particles were used to infect *E. coli* cells. Finally, the beads were resuspended in 100 μl LB broth and incubated at 37°C for 20 min with 100 μl *E. coli* suspension, where the remaining bound phagemid particles were directly adsorbed by the bacteria. The phage-infected *E. coli* cells from the previous steps were plated onto LA plates containing 50 μg/ml ampicillin for overnight culture at 37°C. Single colonies were selected and cultivated with gentle shaking overnight at 37°C in 5 ml LB broth containing 50 μg/ml ampicillin. Phagemids containing a uPAR cDNA fragment were purified using Miniprep kits from QIAGEN (Hilden, Germany), and the sequences of the inserts were determined (SEQLAB, Göttingen, Germany). The following synthetic oligonucleotides were used as primer: 5′-GCC CAG GTG AAA CTG CTC G-3′ and 5′-CAA ACG AAT GGA GAG CCA CC-3′.

Synthesis of Biotinylated uPAR Peptide—The following N-terminally biotinylated peptides were synthesized at Biotrend (Köln, Germany) with purities >95% as determined by HPLC and mass spectrometric analysis:

uPAR-(17–24)	CALGQDLC	(8mer)
uPAR-(66–74)	LTEVVCGLD	(9mer)
uPAR-(84–95)	AVTYSRSRYLEC	(12mer)
uPAR-(108–118)	GRHQSLQCRSP	(11mer)
uPAR-(240–248)	GCATASMCQ	(9mer)

Radiolabeling of Proteins—Soluble uPAR was radiolabeled with $Na^{125}I$ using iodogen pre-coated tubes at a ratio of 100 μCi of $Na^{125}I$/100 μg protein to avoid oxidative damage as described previously (*15*). Free ^{125}I was

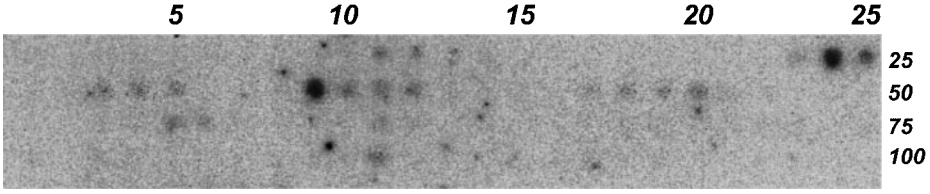

Fig. 2. **Screening of uPAR-binding uPAR fragments by peptide array on SPOT-membrane.** ^{125}I-labeled suPAR was used to bind to a uPAR SPOT-membrane. The peptide spots were numbered as indicated.

```
I                  .....10........20........30
                   |    |    |    |    |    |
uPAR-(7-24)          KTNGDCRVEECALGQDIC
uPAR-(17-28)                  CALGQDICRTTI
SPOT-11                NGDCRVEECALGQDI
SPOT-12                   CRVEECALGQDICRT
SPOT-13                      EECALGQDICRTTIV

                   .....50........60........70
                        |    |    |    |    |
SPOT-23            CTHSEKTNRTLSYRT
SPOT-24               SEKTNRTLSYRTGLK
SPOT-25                  TNRTLSYRTGLKITS

                   60........70........80........90........100...
                   |    |    |    |    |    |    |    |    |
uPAR-(60-75)       GLKITSLTEVVCGLDL
uPAR-(65-102)           SLTEVVCGLDLCNQGNSGRAVTYSRSRYLECISCGSSD
SPOT-28            GLKITSLTEVVCGLD
SPOT-29               ITSLTEVVCGLDLCN
SPOT-30                  LTEVVCGLDLCNQGN
uPAR-(74-91)                        DLCNQGNSGRAVTYSRSR
SPOT-34                                QGNSGRAVTYSRSRY
SPOT-35                                   SGRAVTYSRSRYLEC
SPOT-36                                      AVTYSRSRYLECISC
SPOT-37                                         YSRSRYLECISCGSS

II                 100.......110.......120.......130
                   |    |    |    |    |    |    |
uPAR-(101-121)      SDMSCERGRHQSLQCRSPEEQ
uPAR-(101-121)      SDMSCERGRHQSLQCRSPEEQ
uPAR-(101-117)      SDMSCERGRHQSLQCRS
uPAR-(108-118)           GRHQSLQCRSP
SPOT-42               DMSCERGRHQSLQCR
SPOT-43                  CERGRHQSLQCRSPE
SPOT-44                     GRHQSLQCRSPEEQC
SPOT-45                        QSLQCRSPEEQCLDV

                   140.......150.......160
                   |    |    |    |    |
SPOT-55             DRHLRGCGYLPGCPG
SPOT-56                LRGCGYLPGCPGSNG

                   .....160.......170...
                   |    |    |    |    |
SPOT-61                FHNNDTFHFLKCCNT

III                230.......240.......250.......260...
                   |    |    |    |    |    |    |
uPAR-(234-257)          QSYMVRGCATASMCQHAHLGDAFS
uPAR-(240-248)               GCATASMCQ
uPAR-(240-248)               GCATASMCQ
uPAR-(242-260)                 ATASMCQHAHLGDAFSMNH
SPOT-86                 QSYMVRGCATASMCQ
```

Fig. 3. **Alignment of uPAR-binding uPAR fragments.** Alignment in domain I (A), domain II (B) and domain III (C). Overlapping sequences are boxed.

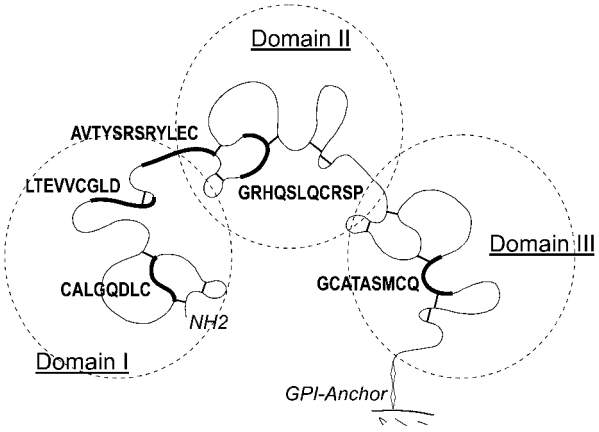

Fig. 4. **Schematic representation of putative uPAR-uPAR interaction sites identified using phage display and peptide array techniques.**

removed by gel filtration on Sephadex G25 (PD-10, Amersham Pharmacia Biotech, Piscataway, NJ). The specific activity of ^{125}I-suPAR was 5–10 × 10^4 cpm/pmole.

Binding of suPAR to a uPAR Peptide Array Synthesized on Cellulose Membrane (SPOT-Membrane)—Fifteen-mer uPAR peptides covering the entire uPAR molecule with twelve amino acid overlap per peptide were directly synthesized as spots on cellulose membranes containing a total of 108 uPAR peptides (kindly provided by Dr. R. Frank, GBF-National Research Center for Biotechnology, Braunschweig, Germany). After extensive washing with PBS, the SPOT-membrane was blocked in 5% skimmed milk in PBST with 0.1% sodium azide overnight at room temperature, and then incubated with ^{125}I-suPAR (10 nM) in fresh blocking buffer for 1 h at room temperature. Binding was detected by autoradiography.

Binding of Biotinylated uPAR-Peptides to uPAR-Transfected BAF-3 Cells—BAF-3 (interleukin-3-dependent mouse B-cell line) cells were from the American Type Culture Collection (ATCC, Rockville, MD), and cultured in RPMI-1640 medium containing 10% fetal calf serum and 2 ng/ml interleukin-3. BAF-3 cells were transfected by electroporation with uPAR cDNA in the sense and antisense orientation using the expression vector pCDNA3. Cells were selected in the presence of G418 (1.2 mg/ml) (Calbiochem, San Diego, CA) and determined to express uPAR by fluorescence-activated cell sorter analysis, Northern blotting and uPAR-enzyme linked immunosorbent assay. The biotinylated uPAR-peptides were each incubated with 50,000 cells at final concentrations of 0.5, 2, 10, or 20 μg/ml in 0.5 ml binding buffer (RPMI-1640 medium containing 0.3% BSA, 2 mM $MgCl_2$ and 2 ng/ml interleukin-3). The mixtures were incubated for 1h at 37°C and 5% CO_2 followed by washing twice with 200 μl binding buffer. Peroxidase-conjugated streptavidin (DAKO, Hamburg, Germany), 1:2000 in binding buffer, was added to the cells, which were further incubated for 1h at room termperature. The cells were washed three times, and bound peroxidase was quantified after 15 min development using 150 μl/well ABTS substrate (Boehringer Mannheim, Mannheim, Germany) with a microplate reader at 405 nm (Molecular Devices, Munich, Germany).

Adhesion of Human U937 Cells to Extracellular Matrix Proteins—The human myelomonocytic U937 cell line was obtained from ATCC and cultured as recommended by the supplier in RPMI-1640 medium containing 10% fetal calf serum. Eighteen hours prior to the experiments, monocytic differentiation was induced by the addition of 50 ng/ml phorbol-12 myristate-13 acetate (PMA, Gibco, Paisley, UK). Ninety-six-well plates were coated with human fibrinogen (20 μg/ml, Kabi-Vitrum, Munich, Germany), fibronectin (20 μg/ml, Sigma, Taufkirchen, Germany) or vitronectin [10 μg/ml, purified from human plasma and converted to the multimeric form as previously described (*16*)] overnight at 4°C and blocked with 3% BSA in Hepes-buffered saline (HBS) for 1 h at room temperature. PMA-stimulated U937 cells were washed in HBS containing 0.3% BSA and mixed with the chromophore BCECF-AM (Molecular Probes, Eugene, OR). After 30 min, the cells were washed and plated onto the precoated wells for 45 min at 37°C in the absence or presence of the uPAR fragments (10 or 50 μM), together with

high molecular weight uPA (50 nM). The adhesion medium was serum free RPMI containing 0.3% BSA or HBS containing 0.3% BSA for adhesion on vitronectin or on fibrinogen and fibronectin, respectively. After the incubation period, total fluorescence of the plates was quantified in a fluorescence plate reader (FLX 800, Bio-Tek Instruments, Winooski, VT). The plates were then washed twice with adhesion buffer to remove non-adherent cells and the remaining fluorescence was measured. Results are expressed as percentage from triplicates performed several times for each experiment.

RESULTS

Mapping of Putative uPAR-uPAR Interaction Sites Using Phage Display—From the suPAR-bound phagemid particles, 30 clones from the pH 5.2 elution, 30 clones from the pH 2.2 elution, and 150 clones from the *E. coli* adsorption were subjected to plasmid extraction and DNA sequencing. All clones were found to contain a uPAR cDNA fragment. Only one of the clones eluted at pH 5.2, uPAR-(60–75), and two of the clones eluted at pH 2.2, uPAR-(101–117) and uPAR-(101–121), had a uPAR peptide sequence, whereas 10 of the 150 clones eluted by *E.coli* adsorption had a correct insert orientation and a correct open reading frame expressing a uPAR fragment. The difference in the probability of uPAR peptide binders among the three elution steps is likely due to the number of clones that were sequenced from each respective elution. The 140 non-uPAR peptides that bound to immobilized uPAR could resist low pH elutions (pH 5.2 and pH 2.2), indicating their binding might not simply be the result of non-specific binding. Further analysis of these peptide sequences may reveal possible uPAR-binding consensus sequences, an approach similar to what we applied earlier (*14*).

In uPAR domain I, overlapping peptides uPAR-(7–24) and uPAR-(17–28), as well as overlapping peptides uPAR-(65–102), uPAR-(74–91) and uPAR-(60–75), bound to suPAR-coated Dynalbeads. In domain II, uPAR-(101–121) was found twice, once in the pH 2.2 elution and once from *E. coli* adsorption, along with two other largely homologous peptides, uPAR-(108–118) and uPAR-(101–117). In domain III, uPAR-(240–248) was found twice to have bound to the suPAR-beads beside two other largely homologous peptides uPAR-(234–257) and uPAR-(242–260). Conceivably, the peptide-clustering regions uPAR-(7–28) and uPAR-(60–91) in domain I, uPAR-(101–121) in domain II and uPAR-(240–260) in domain III are putative uPAR-uPAR contact sites. The results of the analysis and alignment of the suPAR-binding uPAR fragments is presented in Fig. 1, with detailed sequences in Fig. 3. In control experiments, a phage display library containing only vector pComb3B and the *Bst*XI adaptor was mixed with suPAR-coated beads. After washing 10 times with PBST-3% BSA, no phagemid particles were recovered using the elution steps described above.

Screening of uPAR-uPAR Interaction Sites Using SPOT-Membranes—Binding of ^{125}I-suPAR to uPAR peptide array SPOT-membranes revealed several regions that might serve as uPAR-uPAR contact sites. In domain I (Fig. 2 and 3A), SPOTs 11–13 coincided with the uPAR-binding peptides uPAR-(7–24) and uPAR-(17–28) that have the common sequence CALGQDL; SPOT-23, SPOTs-24, and -25, with the common sequence TNRTLSYRT, also bound ^{125}I-suPAR. SPOTs 28–30 coincided with the uPAR-binding peptides uPAR-(60–75) and uPAR-(65–102), which have the common sequence LTEVVCGLD. SPOT-34, which showed a strong signal, along with SPOTs 35–37 share the common sequence YSRSR with the uPAR-binding peptide uPAR-(74–91). In domain II (Figs. 2 and 3B), SPOTs 42–45 covered the same sequence, QSLQCR, as the uPAR-binding peptides uPAR-(101–117), uPAR-(101–121), and uPAR-(108–118). Furthermore, SPOTs-55 and -56, with the common sequence LRGCGYLPGCPG, and SPOT-61 also bound radiolabeled suPAR. In domain III (Figs. 2 and 3C), SPOT 86 had the same sequence, ATASMCQ, as the uPAR-binding peptides uPAR-(234–257), uPAR-(240–248), and uPAR-(242–260). Taken together, the putative uPAR-uPAR interaction sites identified by SPOT-membrane analysis are largely consistent with those identified by phage display.

Binding of Biotinylated Peptides to BAF-3 Cells—Except peptide uPAR-(84–95), which could bind to both wild-type and uPAR-transfected BAF-3 cells, none of the other peptides bound to the uPAR-transfected cells nor the wild type BAF-3 cells (data not shown).

Effect of the Putative uPAR-uPAR Contact Regions on Cell Adhesion—Synthetic peptides uPAR-(84–95) and uPAR-(240–248) could partially inhibit the adhesion of differentiated human U937 monocytes to immobilized Vn in the presence of uPA at two of the tested concentrations. No effect of the synthetic peptides on cell adhesion to vitronectin in the absence of uPA or to fibrinogen and fibronectin was observed (data not shown).

DISCUSSION

Recent findings indicate that uPA-uPAR signaling may play an important role in leukocyte recruitment, angiogenesis, tumor metastasis, inflammation, and vascular remodeling (*2*, *3*). However, how the uPA-uPAR system transduces signals is not fully understood. A major problem is that uPAR has no transmembrane structure; thus, transmembrane adapters may be involved in this process. It is believed that these cellular activities are brought about by the clustering of uPAR with different transmembrane signaling receptors. Typically, uPAR clusters at the cell-substratum interface, at focal adhesion, and at the leading edges of migrating cells, where the direct association of uPAR with integrins has been reported. It has been shown that when suPAR is expressed in and purified from insect cell cultures it may exist as dimers/oligomers, the aggregation possibly representing a natural homophilicity of suPAR (*17*). Further support of the existence of direct homophilic uPAR-uPAR interactions came from our earlier study, where uPA-binding sites containing uPAR peptides could modify the uPAR conformation and affect its interaction with both uPA and Vn (*13*). Yet, it is unknown whether the self-association of uPAR contributes to the control of its bioactivities. The present study was undertaken to determine the uPAR-uPAR contact regions, and to explore possible functions of these regions.

Utilizing the phage display approach, we were able to identify uPA-binding regions in its receptor, and proposed structural requirements for multi-domain binding portions and receptor-receptor interactions (*13*). In the the present study, putative receptor-receptor interaction sites were identified. Four uPAR fragments in domain II and four fragments in domain III within two very short regions were selected, where, strikingly, uPAR-(101–121) and uPAR-(240–248) were found twice each among more than ten million given phagemid particles in the system, demonstrating the highly selective and powerful nature of this technique. Subsequently, these results were further confirmed by the experiments in which suPAR was allowed to bind to an overlapping 15-mer uPAR peptide array. Interestingly, several SPOTs, which apparently bound radiolabeled suPAR, were not found by phage display selection, indicating that larger scale sequencing of bound phagemid particles may provide more comprehensive or additional insight into uPAR-uPAR interactions. Since intact suPAR was used in two independent experimental settings, the identified regions are more likely to represent intermolecular rather than intramolecular contact sites.

It is well estabilised that uPAR is composed of three domains that are thought to share a structure to the Ly-6/uPAR superfamily of GPI-anchored proteins, characterized by a highly conserved spacing and disulfide bonding of cysteine residues. The solution structure of the Ly-6/uPAR member CD59 has been solved by nuclear magnetic resonance (*18*), and confirms a prediction based on a variety of considerations that these proteins share a common structural framework with a large family of structurally defined snake venom α-neurotoxins (*19*). Although definitive proof of this as a model for uPAR awaits its direct structural determination, a further interpretation of our results based on this model may provide useful information regarding uPAR-uPAR interactions. A schematic representation of the putative uPAR-uPAR interaction sites is shown in Fig. 4.

Notably, the uPAR-uPAR interaction sites are completely different from the uPA-binding sites on the uPAR molecule, which were identified earlier using the same approaches. Accordingly, the synthetic uPAR peptides used in this study had no effect on uPA-binding to uPAR (data not shown). However, none of these peptides alone (10 μg/ml) could block ^{125}I-suPAR binding to immobilized uPAR (data not shown). Possibly, uPAR-uPAR homophilic association is an orchestrated action involving multiple contact sites, so that none of the single peptides is able to disrupt the uPAR-uPAR interaction. Furthermore, the observation that only synthetic peptides uPAR-(84–95) and uPAR-(240–248) partially inhibited differentiated human U937 monocyte adhesion to Vn in the presence of uPA, suggests that these two regions might be involved not only in uPAR-uPAR but also in uPAR-Vn interactions. A recent investigation showed that, indeed, uPA regulates Vn binding by controlling uPAR oligomerization (*12*). Biotinylated uPAR peptides containing the putative regions were also tested for binding to uPAR-transfected BAF-3 cells. Except peptide uPAR-(84–95), none of the other peptides bound to the uPAR-transfected cells, suggesting that the uPAR-uPAR homophilic interaction might already have occurred upon uPAR expression on the cell surface. Interestingly, the migration inducing peptide uPAR-(88–95) could bind to murine BAF-3 cells independently from uPAR transfection, suggesting that novel structure(s) on the cell surface may recognize this peptide. A recent study showed that uPAR can activate the G protein-coupled chemotactic receptor FPRL1/LXA4R, and a truncated form of uPAR (amino acids 88–274) can bind directly to FPRL1/LXA4R (*20*). Further investigation is needed to clarify whether uPAR-(88–95) might interact directly with FPRL1/LXA4R. Taken together, we propose that the direct uPAR-uPAR ectodomain interaction is a key determinant in the regulation of various functions of uPAR.

We wish to thank Horst Thiele for skilful technical assistance. This work was supported in part by a grant from the Novartis Foundation, Nürnberg, Germany to K.T.P.

REFERENCES

1. Mondino, A., Resnati, M., and Blasi, F. (1999) Structure and function of the urokinase receptor. *Thromb. Haemost.* **82**, 19–22
2. Blasi, F. and Carmeliet, P. (2002) uPAR: a versatile signalling orchestrator. *Nat. Rev. Mol. Cell. Biol.* **3**, 932–943
3. Chavakis, T., Kanse, S.M., May, A.E., and Preissner, K.T. (2002) Haemostatic factors occupy new territory: the role of the urokinase receptor system and kininogen in inflammation. *Biochem. Soc. Trans* **30**, 168–173
4. Wei, Y., Lukashev, M., Simon, D.I., Bodary, S.C., Rosenberg, S., Doyle, M.V., and Chapman, H.A. (1996) Regulation of integrin function by the urokinase receptor. *Science* **273**, 1551–1555
5. Ossowski, L. and Aguirre-Ghiso, J.A. (2000) Urokinase receptor and integrin partnership: coordination of signaling for cell adhesion, migration and growth. *Curr. Opin. Cell Biol.* **12**, 613–620
6. Chapman, H.A. and Wei, Y. (2001) Protease crosstalk with integrins: the urokinase receptor paradigm. *Thromb. Haemost.* **86**, 124–129
7. Tarui, T., Mazar, A.P., Cines, D.B., and Takada, Y. (2001) Urokinase-type plasminogen activator receptor (CD87) is a ligand for integrins and mediates cell-cell interaction. *J. Biol. Chem.* **276**, 3983–3990
8. Wei, Y., Yang, X., Liu, Q., Wilkins, J.A., and Chapman, H.A. (1999) A role for caveolin and the urokinase receptor in integrin-mediated adhesion and signaling. *J. Cell Biol.* **144**, 1285–1294
9. Preissner, K.T., Kanse, S.M., and May, A.E. (2000) Urokinase receptor: a molecular organizer in cellular communication. *Curr. Opin. Cell. Biol.* **12**, 621–628
10. Koshelnick, Y., Ehart, M., Hufnagl, P., Heinrich, P.C., and Binder, B.R. (1997) Urokinase receptor is associated with the components of the JAK1/STAT1 signaling pathway and leads to activation of this pathway upon receptor clustering in the human kidney epithelial tumor cell line TCL-598. *J. Biol. Chem.* **272**, 28563–28567
11. Sitrin, R.G., Pan, P.M., Harper, H.A., Todd, R.F. 3rd, Harsh, D.M., and Blackwood, R.A. (2000) Clustering of urokinase receptors (uPAR; CD87) induces proinflammatory signaling in human polymorphonuclear neutrophils. *J. Immunol.* **165**, 3341–3349
12. Sidenius, N., Andolfo, A., Fesce, R., and Blasi, F. (2002) Urokinase regulates vitronectin binding by controlling urokinase receptor oligomerization. *J. Biol. Chem.* **277**, 27982–27990
13. Liang, O.D., Chavakis, T., Kanse, S.M., and Preissner, K.T. (2001) Ligand binding regions in the receptor for urokinase-type plasminogen activator. *J. Biol. Chem.* **276**, 28946–28953
14. Liang, O.D., Chavakis, T., Linder, M., Bdeir, K., Kuo, A., and Preissner, K.T. (2003) Binding of urokinase plasminogen acti-

vator to gp130 *via* a putative urokinase-binding consensus sequence. *Biol. Chem.* **384**, 229–236
15. Bdeir, K., Kuo, A., Mazar, A., Sachais, B.S., Xiao, W., Gawlak, S., Harris, S., Higazi, A.A., and Cines, D.B. (2000) A region in domain II of the urokinase receptor required for urokinase binding. *J. Biol. Chem.* **275**, 28532–28538
16. Stockmann, A., Hess, S., DeClerck, P., Timpl, R., and Preissner, K.T. (1993) Multimeric vitronectin. Identification and characterization of conformation-dependent self-association of the adhesive protein. *J. Biol. Chem.* **268**, 22874–22882
17. Shliom, O., Huang, M., Sachais, B., Kuo, A., Weisel, J.W., Nagaswami, C., Nassar, T., Bdeir, K., Hiss, E., Gawlak, S., Harris, S., Mazar, A., and Higazi, A.A. (2000) Novel interactions between urokinase and its receptor. *J. Biol. Chem.* **275**, 24304–24312
18. Fletcher, C.M., Harrison, R.A., Lachmann, P.J., and Neuhaus, D. (1994) Structure of a soluble, glycosylated form of the human complement regulatory protein CD59. *Structure* **2**, 185–199
19. Ploug, M. and Ellis, V. (1994) Structure-function relationships in the receptor for urokinase-type plasminogen activator. Comparison to other members of the Ly-6 family and snake venom alpha-neurotoxins. *FEBS Lett.* **349**, 163–168
20. Resnati, M., Pallavicini, I., Wang, J.M., Oppenheim, J., Serhan, C.N., Romano, M., and Blasi, F. (2002) The fibrinolytic receptor for urokinase activates the G protein-coupled chemotactic receptor FPRL1/LXA4R. *Proc. Natl Acad. Sci. USA* **99**, 1359–1364